IR SINGLE-PHOTON RECIEVER BASED ON ULTRATHIN NbN SUPERCONDUCTING FILM

A. A. Korneev[1], A. V. Divochiy[1,2], Yu. B. Vakhtomin[2], Yu. P. Korneeva[1], P. A. Larionov[1], N. N. Manova[1], I. N. Florya[1], A. V. Trifonov[1,3], B. M. Voronov[1], K. V. Smirnov[1,2], A. V. Semenov[1], G. M. Chulkova[1,3], G. N. Goltsman[1,2]

[1] Moscow State Pedagogical University
[2] CJSC "Superconducting nanotechnology"
[3] Nizhny Novgorod State Technical University n.a. R.E. Alekseev

Abstract. We present our recent results in research and development of superconducting single-photon detector (SSPD). We achieved the following performance improvement: first, we developed and characterized SSPD integrated in optical cavity and enabling its illumination from the face side, not through the substrate, second, we improved the quantum efficiency of the SSPD at around 3 μm wavelength by reduction of the strip width to 40 nm, and, finally, we improved the detection efficiency of the SSPD-based single-photon receiver system up to 20% at 1550 nm and extended its wavelength range beyond 1800 nm by the usage of the fluoride ZBLAN fibres.

Keywords: Infrared single-photon detectors, superconducting thin film device fabrication, NbN films.

The state-of-the-art quantum optics experiments require efficient and fast single-photon detectors with low dark counts rate, and picosecond timing resolution (jitter). It is also very favorable for the detector to be capable to operate both in visible and infrared including the wavelengths longer than 1.8 μm, a limit for widely used InGaAs avalanche single-photon diodes.

One of the novel single-photon detectors is superconducting single-photon detector based 100-nm-wide meander-shaped NbN strip. The operation principle of such a detector is based on the local suppression of the superconductivity in the strip and formation of a resistive barrier [1,2]. Recently several new modifications were

introduced: photon-number resolving SSPD [3], SSPD with wires connected in parallel [4-6], SSPD integrated with optical cavities [7-10]. Here we present an overview of our recent research results on SSPD and its application in a practical single-photon receiver system.

Our recent research was inspired by the need of the practical application of the SSPD. As the ultimate detection efficiency is limited by the NbN film absorption the straightforward way to overcome this limitation is to integrate the SSPD with a quarter-wave optical microcavity. Previously reported realizations [7,8] featured the microcavity fabricated on the face side of the detector, i.e. the NbN film was deposited and patterned on the substrate, then a $\lambda/4$ dielectric layer was deposited on the patterned NbN film and finally the metallic mirror was placed on top of the dielectric layer. Although being reported above 60% quantum efficiency [8] such a detector is very difficult in practical usage: typically the light is fed to the SSPD by a single-mode optical fibre connected directly to the NbN meander. Cavity-integrated SSPDs require illumination through the substrate which in its turn require elaborated optics (lensed fibres, etc) and alignment techniques (such as active probe station).

Another approach was introduced in [9], i.e. to fabricate SSPD on Si substrate with SiO_2 layer. The Si/SiO_2 interface acted as a mirror. Although this approach gives a noticeable improvement in quantum efficiency it does not allow one to reach an ultimate almost unity absorption due to a relatively low reflectivity of this interface.

We managed to fabricate a cavity-integrated SSPD suitable for illumination from the face side thus enabling simple packaging with optical fibres. Our detector included a metal mirror with high reflectivity prospective for achieving near 100% quantum efficiency. We started with a patterning of the metal mirror on the sapphire substrate (Fig. 1). First we deposited Au-Nb layer by DC magnetron sputtering (5-nm-thick Nb layer was used to provide a good adhesion, Au thickness was 70 nm). Then we exposed photoresist AZ1512 all around the future mirror. The exposed resist was removed and then all unnecessary Au-Nb film was removed by wet etching from everywhere except the mirror. Then we deposited 75-nm-thick layer of Al_2O_3 to make it of the same thickness as the mirror. This layer was deposited by e-beam

evaporation. Afterwards we removed Al$_2$O$_3$ layer from the mirror by the lift-off process using the layer of photoresist AZ1512 that remained on the mirror after the previous step. Now we deposited λ/4 layer of SiO by e-beam evaporation as well and then we deposited NbN layer by DC reactive magnetron sputtering and patterned it in the same way we do for usual SSPD on sapphire substrate [11].
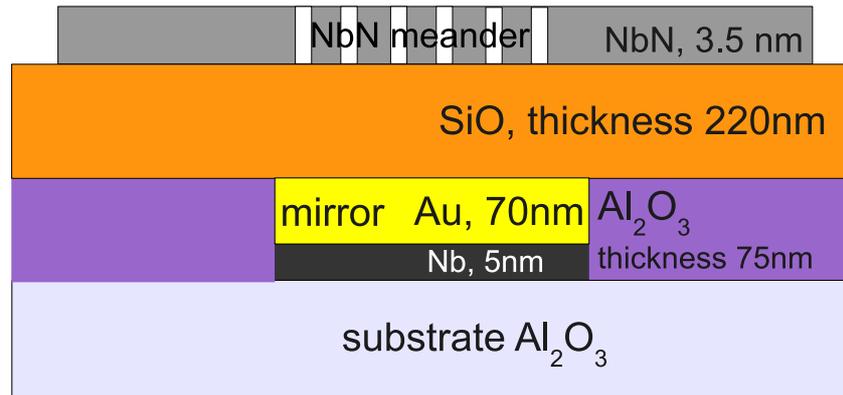
Fig. 1. A schematic drawing of the cavity-integrated SSPD cross-section.
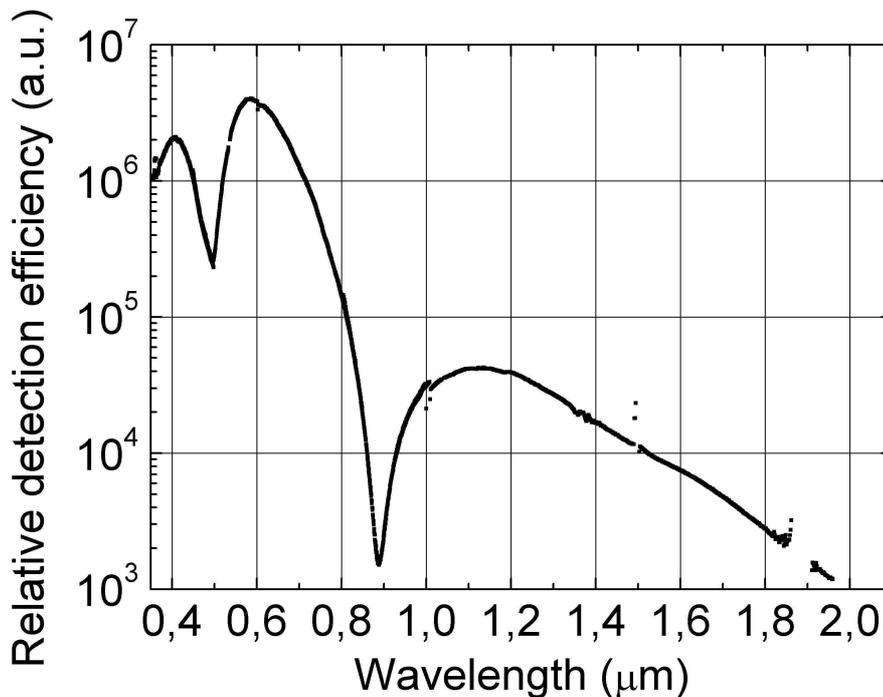
Fig. 2. "Relative" quantum efficiency of the cavity-integrated SSPD.

We characterized the spectral sensitivity of the fabricated devices in the wavelength range from 400 nm to 2000 nm. As a light source we used a grating spectrometer. The SSPD was installed in a liquid helium optical cryostat and maintained at about 3K temperature. The light count rate was measured at bias current corresponding to 10 dark counts per second. Then, at each wavelength we measured the light power, thus we obtained the "relative" quantum efficiency by dividing the SSPD count rate at a given wavelength to the number of photons obtained from the power measurement. It is "relative" as we were not able to measure the exact number of photons falling on the SSPD but only the ratio of the photon fluxes at different wavelengths. The result is presented in Fig. 2. One can observe maximums and minimums of quantum efficiency caused by constructive and destructive interference.

Many practical applications require a fast detector with single-photon sensitivity beyond 1.8 μm where there is a lack of practical single-photon detectors. To improve the sensitivity of the SSPD we managed to reduce the strip width down to 40 nm. For this we used electron resist ZEP 520 instead of PMMA 950K that we used before. The reduction of the strip width leads to the reduction of the response voltage, thus we decided to connect many superconducting strips in parallel utilizing a cascade switching mechanism [4,5] for response signal amplification. This novel device, a parallel-wire SSPD, consisted of 53 parallel wires, each 40-nm-wide with the gap between the wires of 90 nm. The total area of the device was 7 μm × 7 μm. We measured the spectral sensitivity of such a device in wavelength range 1 μm to 3.5 μm and compared it with a usual meander. The measurement was performed in the optical liquid helium cryostat at 3 K temperature. First we measured a relative quantum efficiency in the same way as we did for cavity-integrated devices described above. Then we measured quantum efficiency of this device at 1.3 μm wavelength in a fibre-coupled set-up. Thus we were able to retrieve absolute quantum efficiencies. Fig. 3 presents a spectral sensitivity of a parallel-wire SSPD with 40-nm-wide strip in wavelength range 1 μm to 3.5 μm in comparison with a usual SSPD with 104-nm-wide strip. Both devices were biased with the current corresponding to 20~kHz of dark counts rate. One can see that although parallel-wire device exhibited smaller

quantum efficiency in near infrared (around 1 μm), at 3.5 μm it had about an order of magnitude better efficiency compared to the usual meander device.
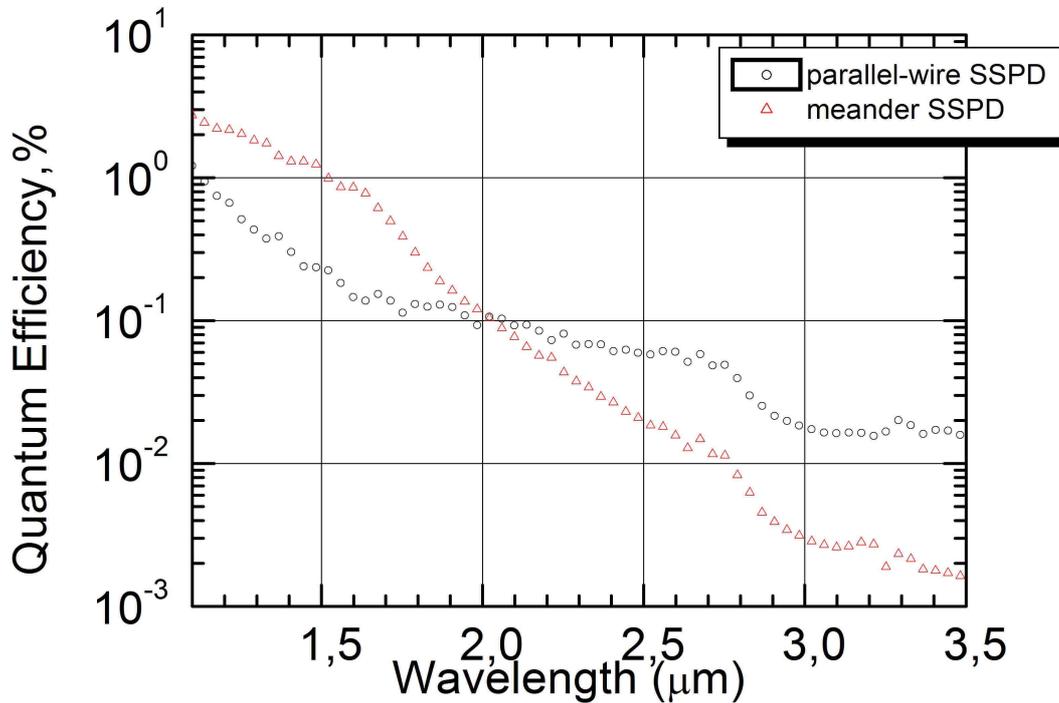
Fig. 3. Quantum efficiency vs wavelength for parallel-wire SSPD and usual meander SSPD.

Finally, we managed to improve the quantum efficiency of the usual meander-shaped SSPD and used them in a single-photon receiver system. We characterized the detection efficiency of the receiver in range 600 nm – 2000 nm with different single-mode fibres: HP780, SMF-28e XB, and ZBLAN.

As the SSPD's quantum efficiency increases with the temperature reduction and almost reaches its saturation value at about 2 K temperature we designed the receiver system for enabling SSPD operation at 2 K temperature in a standard storage dewar. The receiver system was designed as a double-wall insert with vacuum insulation. Liquid helium from the storage dewar penetrated into the inner volume of the insert through the capillary located at the bottom of the insert. The reduction of the temperature to 2 K level was achieved by helium vapour pumping from the insert inner volume. The capillary limited the speed of liquid helium penetration and allowed for obtaining a vapor pressure of 80-120 Pa and a temperature of 1.7 K. The

minimum achievable temperature is mostly determined by the capabilities of the pump and can be as low as 1.6 K. Temperature below 2 K can be achieved with a pump performance above 5 m^3/hour.

The SSPD was coupled to the optical fibre by precision alignment against the fibre core and subsequent mechanical fixing in a specially designed mount. Being cooled down to ~ 2K the SSPD did not exhibit any noticeable misalignment. We used three types of fibres for different wavelength ranges. In the range 600 nm – 1600 nm we used SSPD with the HP780 fibre which is single-mode for visible light. In the range 1000 nm – 1800 nm we used SMF-28e XB fibre which is a typical single-mode fibre for telecom wavelengths of 1300 nm and 1550 nm. Finally we used fluoride ZBLAN fibre to characterize the receiver at 1800 nm wavelength which is beyond the transparency window of the silica.

We determine detection efficiency as the ratio of the number detector counts to the number of photons at the fibre input of the receiver. At each measured wavelength we obtained the number of photons from the optical power measurement.
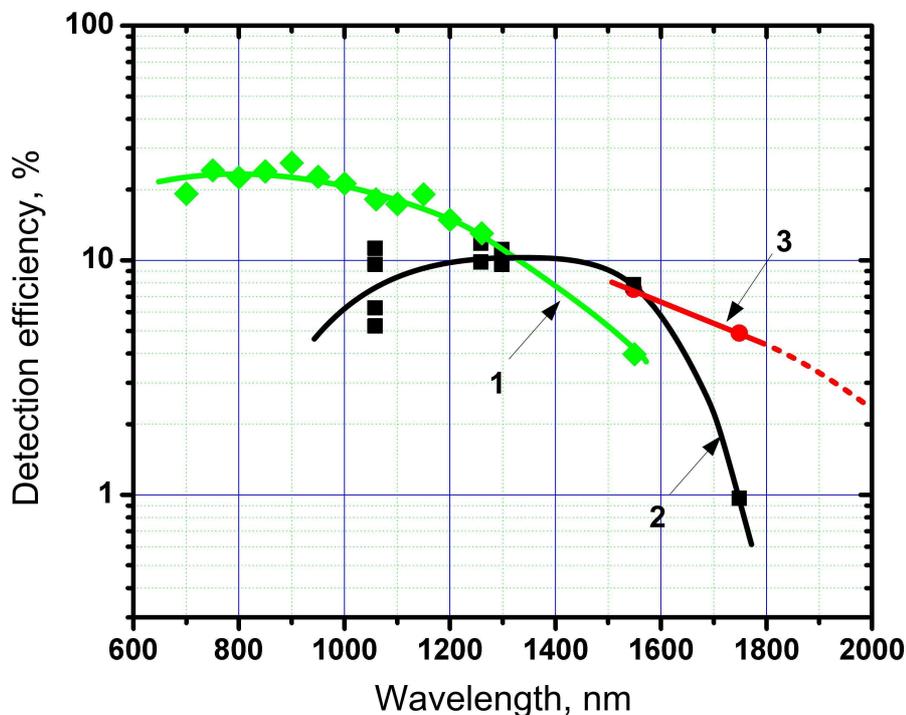
Fig.4. Detection efficiency of the single photon receiver measured in wavelength range from 600 nm – 1800 nm with three different fibres: (1) HP780, (2) SMF-28e XB, and (3) ZBLAN fibre based on fluoride glass transparent beyond 1800 nm.

Figure 4 presents system quantum efficiency measured in range from 800 nm to 1800 nm with different optical fibres. One can see that the application of ZBLAN fibre enabled us to extend the spectral operation range beyond 1.7 μm, a cut-off for standard silica fibres. One can see that at 1750 nm wavelength on ZBLAN fibre quantum efficiency is as high as 5%. Such a detector was successfully used for the research into quantum dot emission near 2 μm wavelength [12].

In conclusion, we presented the results of our recent efforts to improve SSPD's quantum efficiency and promote them to longer wavelength range. First we managed to fabricate a cavity-integrated SSPD compatible with coupling to the single-mode fibre and observed an improvement of the quantum efficiency at the target wavelength due to constructive interference of the incident and reflected waves. Second, we developed the SSPD with 40-nm-wide strip instead of typical 100 nm and demonstrated its better quantum efficiency at 3-3.5 μm wavelengths compared to SSPD with 100-nm-wide strip. And finally we improved the performance of the single-photon receiver based on the traditional meander-shaped SSPDs, i.e. due to improved SSPD the receiver demonstrates up to 20% detection efficiency (reduced to the receiver input) at 1550 nm at 10 dark counts per second, and we extended the wavelength range of the receiver beyond 1800 nm by the usage of fluoride-based ZBLAN fibres.

References

1. G. Gol'tsman, O. Okunev, G. Chulkova, A. Lipatov, A. Semenov, K. Smirnov, B. Voronov, A. Dzardanov, C. Williams, R. Sobolewski, Appl. Phys. Lett. 79, 705 (2001).

2.   A. Semenov, G. Gol'tsman, A. Korneev, Physica C 352, 349 (2001).

3. A. Divochiy, F. Marsili, D. Bitauld, A. Gaggero, R. Leoni, F. Mattioli, A. Korneev, V. Seleznev, N. Kaurova, O. Minaeva, G. Goltsman, K.G. Lagoudakis, M. Benkhaoul, F. L´evy, A. Fiore, Nature Photonics 2, 302 (2008).

4. M. Ejrnaes, R. Cristiano, O. Quaranta, S. Pagano, A. Gaggero, F. Mattioli, R. Leoni, B. Voronov, G. Goltsman, Appl. Phys. Lett. 91, 262509 (2007).

5. F. Marsili, F. Najaf, E. Dauler, F. Bellei, X. Hu, M. Csete, R.J. Molnar, K.K. Berggren, Nano Lett. 11(5), 20482053 (2011).

6. Y. Korneeva, I. Florya, A. Semenov, A. Korneev, G. Goltsman, Applied Superconductivity, IEEE Transactions on 21, 323 (2011).

7. I. Milostnaya, A. Korneev, I. Rubtsova, V. Seleznev, O. Minaeva, G. Chulkova, O. Okunev, B. Voronov, K. Smirnov, G. Gol'tsman, W. S lysz, M. Wegrzecki, M. Guziewicz, J. Bar, M. Gorska, A. Pearlman, J. Kitaygorsky, A. Cross, R. Sobolewski, Journal of Physics: Conference Series 43, 1334 (2006).

8. K. Rosfjord, J. Yang, E. Dauler, A. Kerman, V. Anant, B. Voronov, G. Goltsman, K. Berggren, Optics Express 14(2), 527 (2006).

9. M.G. Tanner, C.M. Natarajan, V.K. Pottapenjara, J.A. O'Connor, R.J. Warburton, R.H. Hadfield, B. Baek, S. Nam, S.N. Dorenbos, E.B. Ure˜na, T. Zijlstra, T.M. Klapwijk, V. Zwiller, Appl. Phys. Lett. 96, 221109 (2010).

10. A. Gaggero, S.J. Nejad, F. Marsili, F. Mattioli, R. Leoni, D. Bitauld, D. Sahin, G.J. Hamhuis, R. N¨otzel, R. Sanjines, A. Fiore, Appl. Phys. Lett. 97(15), 151108 (2010).

11. G. Gol'tsman, K. Smirnov, P. Kouminov, B. Voronov, N. Kaurova, V. Drakinsky, J. Zhang, A. Verevkin, R. Sobolewski, IEEE Transactions On Applied Superconductivity 13(2), 192 (2003).

12. D. Elvira, A. Michon, B. Fain, G. Patriarche, G. Beaudoin, I. Robert-Philip, Y. Vachtomin, A.V. Divochiy, K.V. Smirnov, G.N. Goltsman, I. Sagnes, A. Beveratos, Appl. Phys. Lett. 97, 131907 (2010).